

Thermodynamic Analogy for Structural Phase Transitions

Pavel Cejnar^{*}, Stefan Heinze[†] and Jan Dobeš^{**}

^{*}*Institute of Particle and Nuclear Physics, Charles University, V Holešovičkách 2, 180 00 Prague, Czech Rep.*

[†]*Institute of Nuclear Physics, University of Cologne, Zùlpicherstrasse 77, 50937 Cologne, Germany*

^{**}*Nuclear Physics Institute, Academy of Sciences of the Czech Republic, 250 68 Řež, Czech Rep.*

Abstract. We investigate the relationship between ground-state (zero-temperature) quantum phase transitions in systems with variable Hamiltonian parameters and classical (temperature-driven) phase transitions in standard thermodynamics. An analogy is found between (i) phase-transitional distributions of the ground-state related branch points of quantum Hamiltonians in the complex parameter plane and (ii) distributions of zeros of classical partition functions in complex temperatures. Our approach properly describes the first- and second-order quantum phase transitions in the interacting boson model and can be generalized to finite temperatures.

INTRODUCTION

Quantum structural phase transitions (QPT's) at zero temperature are well known in both lattice [1] and many-body systems [2]–[24]. In any of such transitions, the structure of the ground state (and few low-lying states) does not evolve smoothly with the Hamiltonian control parameters, but flips abruptly from one configuration to another at a certain “critical point”. A typical QPT Hamiltonian reads as

$$H(\lambda) = H_0 + \lambda V = (1 - \lambda)H(0) + \lambda H(1), \quad (1)$$

where H_0 and V represent two incompatible terms, $[H_0, V] \neq 0$, and λ is a dimensionless control parameter. Since arbitrary scaling and sign factors can be absorbed in V , one can require $\lambda \in [0, 1]$. The variation of λ drives the system between two limiting $\lambda = 0$ and $\lambda = 1$ modes of motions, which are in the many-body case typically associated with spherical and deformed shapes of nuclei [3, 7, 9, 11, 14, 15, 21, 23], paired and unpaired phases of strongly interacting Fermi systems [5, 6, 8, 17], or with normal and superradiant modes of some quantum optical systems [18].

For $|\lambda|$ large enough, the term λV in Eq. (1) prevails over H_0 and the spectrum of $H(\lambda)$ just freely expands. The most interesting physics thus happens around the minimum λ_0 of the parabola that for finite Hilbert-space dimensions n determines the dispersion $\Delta^2 E = n^{-1} \text{tr} H^2 - n^{-2} \text{tr}^2 H$ of energies in the spectrum as a function of λ . The ground-state (g.s.) related structural phase transitions (if any) most typically appear at a critical value λ_c not far away from λ_0 . They can be observed by analyzing the average

$$\langle V \rangle_0 \equiv \langle \Psi_0 | V | \Psi_0 \rangle = \frac{dE_0}{d\lambda}, \quad (2)$$

where $E_0(\lambda)$ is the energy and $|\Psi_0(\lambda)\rangle$ the normalized eigenvector of the ground state. It can be shown that $\langle V \rangle_0$ is a nonincreasing function of λ , which in the QPT case develops either a discontinuity or nonanalyticity at λ_c . The $n \rightarrow \infty$ limit is usually required for a QPT to occur (diagonalization of a finite- n Hamiltonian cannot generate a nonanalytic behavior), but distinctive QPT precursors can be often observed already in moderate dimensions. (Note, however, that a discontinuous change of the $\langle V \rangle_0$ can take place even in finite- n cases if the ground state undergoes an unavoided crossing with another state [19].) If the $(\kappa - 1)$ th derivative of $\langle V \rangle_0$ is discontinuous at λ_c , the derivatives of E_0 are discontinuous (singular) starting from the κ th one. This situation is described as a QPT of order κ [2, 4], in analogy with the well-known Ehrenfest classification of thermodynamic phase transitions.

Of particular interest are the situations when $\langle V \rangle_0$ drops to zero and, simultaneously, also the dispersion, $\langle V^2 \rangle_0$, vanishes at the critical point. Typically, this may happen if V is semi-positively definite. Consequently, $\langle V \rangle_0$ must remain zero for all $\lambda \geq \lambda_c$ and the g.s. wave function gets fixed (in the non-degenerate case). In these cases $\langle V \rangle_0$ may

be considered as an “order parameter” that distinguishes two quantum “phases” of the model (the values $\langle V \rangle_0 = 0$ and $\langle V \rangle_0 \neq 0$ being attributed to “more symmetric” and “less symmetric” phases, respectively).

The ground-state QPT’s happen at temperature $T = 0$ and thus have no real thermal attributes. Therefore, questions often arise whether the term “phase transition” used in this context is just a metaphor, or whether it refers to some deeper analogies in standard thermodynamics [25]. Of course, the situation becomes more general if the system is described with both λ and T taken as free parameters. The g.s. average $\langle V \rangle_0$ is then replaced by a thermal average

$$\langle V' \rangle_T \equiv \frac{\text{tr}(V' e^{-T^{-1}H})}{\text{tr} e^{-T^{-1}H}} = \frac{\partial F_0}{\partial \lambda}, \quad (3)$$

where $F_0(\lambda, T) = -T \ln \text{tr} e^{-T^{-1}H(\lambda)}$ is the equilibrium value of the free energy and $V' = -T \left[\frac{\partial}{\partial \lambda} e^{-T^{-1}H(\lambda)} \right] e^{T^{-1}H(\lambda)}$ an operator generating the finite-temperature “order parameter” (one can prove that $\langle V' \rangle_T \rightarrow \langle V \rangle_0$ for $T \rightarrow 0$). In this case, both structural (driven by λ) and thermodynamic (driven by T) phase transitions turn out to be just two different aspects of the same phenomenon, residing in the full $\lambda \times T$ parameter space [1, 2], and a common language should be developed for their description.

In this contribution, we will mostly deal only with the simplest case, i.e., with the $T = 0$ limit of quantum phase transitions. The approach [24] will be presented that makes it possible to treat such transitions fully in parallel with thermodynamic phase transitions at finite temperatures. This approach is based on a similarity between the distribution of zeros of the partition function Z at complex temperatures for systems undergoing classical phase transitions [26, 27] and the distribution of so-called branch points of QPT Hamiltonians (1) in complex-extended λ plane [6]. Since a generalization of our method to finite temperatures seems possible, we believe that it represents the right way toward the unified description of quantum phase transitions in the $\lambda \times T$ space.

QPT’S IN THE INTERACTING BOSON MODEL

As a testing ground, we will use the interacting boson model (IBM) [28], well known from nuclear-structure studies as well as from analyses focused on general features of quantum chaos and quantum phase transitions. This model describes nuclear shapes and collective motions in terms of an ensemble of N interacting s and d bosons with angular momenta 0 and 2, respectively. Its algebraic formulation is based on the dynamical algebra $U(6)$ formed by 36 bilinear products $b_i^\dagger b_j$ of boson creation and annihilation operators, where $b_i = s$ or d_μ with $\mu = -2, \dots, +2$. This allows one to extract several alternative dynamical symmetries and find analytic solutions for the corresponding Hamiltonians. All the IBM dynamical symmetries lead to the algebra $O(3)$ of angular momentum $L = \sqrt{10}(d^\dagger d)^{(1)}$ which guarantees the invariant symmetry of the model under rotations.

Individual dynamical symmetries are named after the first algebras in the respective $U(6) \supset \dots \supset O(3)$ decompositions, so we have $U(5)$, $SU(3)$, $O(6)$, $\overline{SU(3)}$, and $\overline{O(6)}$ dynamical symmetries (the fourth and fifth chain differs from the second and third one, respectively, just by relative phases between s and d bosons in definitions of the corresponding algebras). Both first- and second-order QPT’s—according to the Ehrenfest classification—are present in the IBM parameter space between these symmetries. Since geometry can be attributed to given algebraic structures via the coherent state formalism, the IBM phase transitions describe changes of the nuclear ground-state shapes. In particular, using the projected coherent states [29]

$$|N, \beta, \gamma\rangle \propto \left(s^\dagger + \beta \cos \gamma d_0^\dagger + \frac{\beta \sin \gamma}{\sqrt{2}} [d_{-2}^\dagger + d_{+2}^\dagger] \right)^N |0\rangle \quad (4)$$

with β and γ interpreted as Bohr geometric variables, one obtains the following shape types associated with individual dynamical symmetries: spherical [$U(5)$], prolate [$SU(3)$], oblate [$\overline{SU(3)}$], and deformed γ -soft [$O(6)$, $\overline{O(6)}$].

The IBM Hamiltonian is assumed to have a general form containing one- and two-body terms, with few restrictions resulting from fundamental symmetry requirements. This leads to the most general Hamiltonian with six free parameters (except an additive constant). However, a more involved analysis focused on phase-transitional properties [7] reveals that there are only two essential parameters. An archetypal two-parameter Hamiltonian (see, e.g., Refs. [10, 13]) reads as

$$H_\chi(\lambda) = (1 - \lambda) \left[-\frac{Q_\chi \cdot Q_\chi}{N} \right] + \lambda n_d, \quad (5)$$

where the parameters change within domains $\lambda \in [0, 1]$ and $\chi \in [-\frac{\sqrt{7}}{2}, \frac{\sqrt{7}}{2}]$, while $n_d = d^\dagger \cdot \tilde{d}$ represents the d -boson number operator and $\mathcal{Q}_\chi = d^\dagger \tilde{s} + s^\dagger \tilde{d} + \chi(d^\dagger \tilde{d})^{(2)}$ the quadrupole operator. The U(5) dynamical symmetry is located at $\eta = 1$ and χ arbitrary, O(6) at $(\eta, \chi) = (0, 0)$, SU(3) and $\overline{\text{SU}}(3)$ at $(\eta, \chi) = (0, -\frac{\sqrt{7}}{2})$ and $(0, +\frac{\sqrt{7}}{2})$, respectively, while $\overline{\text{O}}(6)$ is absent in the given parametrization.

Clearly, if χ is fixed to a constant, the Hamiltonian in Eq. (5) has the general form (1) with

$$V = n_d + \frac{\mathcal{Q}_\chi \cdot \mathcal{Q}_\chi}{N} \quad (6)$$

being a semi-positive operator. It is not difficult to see that $\langle V \rangle_0 > 0$ for $\lambda = 0$ and $\langle V \rangle_0 = 0$ for $\lambda = 1$, so the scenario described in the previous section may be expected to apply in the $N \rightarrow \infty$ limit. Indeed, the order parameter can be expressed in terms of the Bohr deformation parameters β_0 and γ_0 , resulting from minimization of the coherent-state energy functional

$$\mathcal{E}(\lambda, \chi; \beta, \gamma) \equiv \lim_{N \rightarrow \infty} \frac{1}{N} \langle H_\chi(\lambda) \rangle_{|N, \beta, \gamma} = \frac{(5\lambda - 4)\beta^2 + 4\sqrt{\frac{2}{7}}(1 - \lambda)\beta^3 \cos 3\gamma + [\lambda - \frac{2}{7}\chi^2(1 - \lambda)]\beta^4}{(1 + \beta^2)^2} \quad (7)$$

(normalization per boson is included to ensure finite $N \rightarrow \infty$ asymptotics), namely

$$\langle \mathcal{V} \rangle_0 \equiv \lim_{N \rightarrow \infty} \frac{1}{N} \langle V \rangle_0 = \frac{5\beta_0^2 - 4\sqrt{\frac{2}{7}}\chi\beta_0^3 \cos 3\gamma_0 + (\frac{2}{7}\chi^2 + 1)\beta_0^4}{(1 + \beta_0^2)^2}. \quad (8)$$

For $\chi \neq 0$, the value of β_0 changes from $\beta_0 \neq 0$ to 0 at

$$\lambda_c = \frac{4 + \frac{2}{7}\chi^2}{5 + \frac{2}{7}\chi^2}, \quad (9)$$

indicating a first-order deformed-to-spherical QPT (the order parameter $\langle \mathcal{V} \rangle_0$ drops from a positive value to zero). For $\chi = 0$, the value $\beta_0 \propto \sqrt{\lambda_c - \lambda}$ valid in the left vicinity of λ_c continuously joins with $\beta_0 = 0$ valid above λ_c ; the corresponding QPT is of the second order, with the critical exponent for $\langle \mathcal{V} \rangle_0$ equal to 1. Because of the proper weighting of both terms in Hamiltonian (5) the finite- N precursors of the QPT behavior are always located in the region around (9), independently of N .

Besides the spherical-deformed phase separatrix, there exists also a separatrix at $\chi = 0$ and $\lambda < \frac{4}{5}$ which corresponds to the first-order QPT between prolate and oblate shapes, where either β_0 changes the sign or, equivalently, γ_0 jumps from 0 to $\frac{\pi}{6}$. In this case, however, the form (1) [with λ replaced by χ , and H_0 and V by the corresponding expressions following from Eq. (5)] can be used only locally, close to $\chi = 0$. We will not be dealing with the prolate-oblate transition here.

An obvious way to classify the IBM deformed-spherical QPT (driven by the interaction parameter λ) relies on the analogy between the $N \rightarrow \infty$ g.s. energy per boson, $\mathcal{E}_0(\lambda, \chi) \equiv \mathcal{E}(\lambda, \chi; \beta_0, \gamma_0)$, as a function of λ , and the equilibrium value of the free energy, $F_0(T)$, as a function of temperature T . This leads to the Ehrenfest classification. Using the standard definition $C = -T \frac{\partial^2 F_0}{\partial T^2}$, one can even introduce a QPT analog of the ‘‘specific heat’’

$$\mathcal{C} = -\lambda \frac{\partial^2 \mathcal{E}_0}{\partial \lambda^2} = -\lambda \frac{\partial \langle \mathcal{V} \rangle_0}{\partial \lambda} = \lim_{N \rightarrow \infty} \frac{2\lambda}{N} \sum_{i>0} \frac{|\langle V \rangle_{0i}|^2}{E_i - E_0} \quad (10)$$

and show that it behaves exactly as expected for a thermodynamic phase transition of the respective order [16]. Here and in the following, $E_i \equiv E_i(\lambda, \chi)$ stands for the i th eigenvalue of $H_\chi(\lambda)$ while $\langle V \rangle_{ij} \equiv \langle \Psi_i(\lambda, \chi) | V | \Psi_j(\lambda, \chi) \rangle$ and $\langle V \rangle_i \equiv \langle V \rangle_{ii}$ denote matrix elements of V involving i th and j th eigenstates. Note that the sum in Eq. (10) runs effectively only over those states that have the same symmetry quantum numbers as the ground state, since otherwise $\langle V \rangle_{0i} = 0$.

ALTERNATIVE DEFINITIONS OF A QPT ‘‘SPECIFIC HEAT’’

It turns out that Eq. (10) does not represent the only form of the QPT analog of specific heat. Inspired by the thermodynamic relation $C = T \frac{\partial}{\partial T} S$, where S is the entropy, one can define $\mathcal{C} = \lambda \frac{\partial}{\partial \lambda} \mathcal{S}$ with $\mathcal{S} = -\sum_i |\langle i | \Psi_0 \rangle|^2 \ln |\langle i | \Psi_0 \rangle|^2$

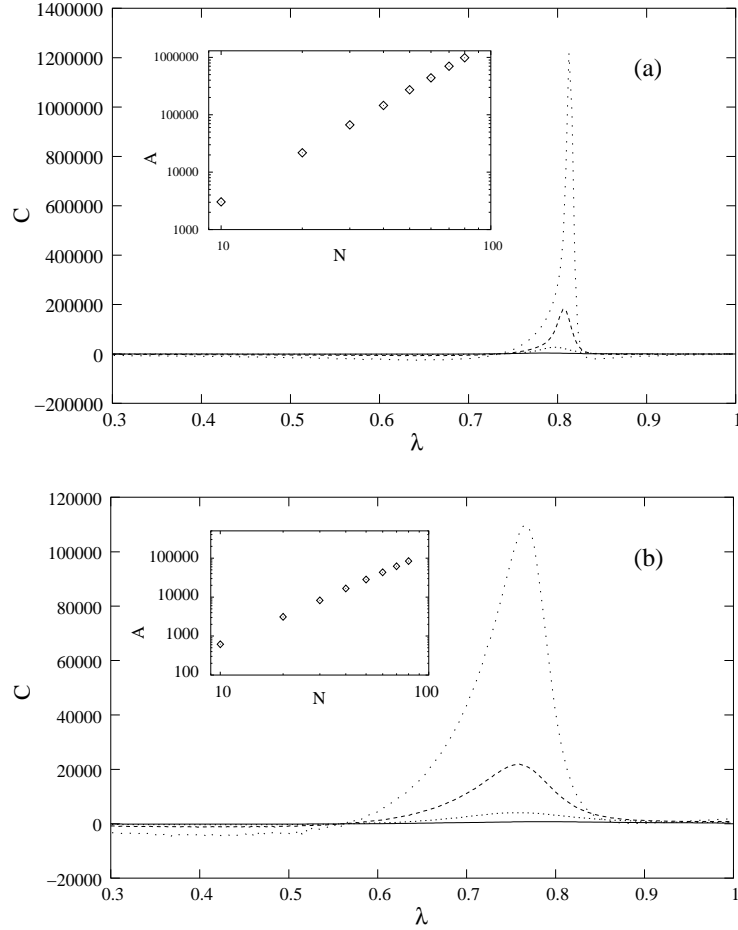


FIGURE 1. “Specific heat” (13) with $\Omega = 1$ including all $J = 0$ states for (a) the first-order and (b) second-order QPT of the interacting boson model [Hamiltonian (5) with (a) $\chi = \pm \frac{\sqrt{7}}{2}$ and (b) $\chi = 0$]. The curves in order from the lowest to the highest correspond to $N = 10, 20, 40,$ and 80 . The insets show the increase of the peak maximal amplitude with N .

being the wave-function entropy of the ground state with respect to the eigenbasis $|i\rangle$ of $H(1)$, i.e., the basis associated with the $U(5)$ dynamical symmetry in our case. This seems to be a plausible alternative definition of specific heat [16] for systems where $\langle V \rangle_0$ and $\langle V^2 \rangle_0$ drop to zero at λ_c . (Note that λ should be inverted here to $\tilde{\lambda} = 1 - \lambda$ in order that the entropy \mathcal{S} increases with “temperature” $\tilde{\lambda}$.)

Another possibility is to randomize Hamiltonian (1) by adding a small stochastic component $\delta\lambda$ to the control parameter (with $\langle \delta\lambda \rangle = 0$ and $\langle \delta\lambda^2 \rangle \equiv \sigma^2 \ll 1$) and to exploit the perturbative expansion $H(\lambda + \delta\lambda) = H(\lambda) + (\delta\lambda)V$. In this way, the ground state wave-function transforms into a density operator $\rho_0(\lambda)$, whose identification with a canonical ensemble provides a natural basis for a noise-induced thermalization of the given quantum system. The resulting specific heat reads as

$$\mathcal{C} = \text{tr}(\rho_0 \ln^2 \rho_0) - \text{tr}^2(\rho_0 \ln \rho_0) \approx (\sigma^2 \ln^2 \sigma^2) \sum_{i>0} \frac{|\langle V \rangle_{0i}|^2}{(E_i - E_0)^2}, \quad (11)$$

where the last equality is valid for very small values of σ^2 (in the IBM, a natural scaling of σ^2 for $N \rightarrow \infty$ is $\sigma^2 \propto N^{-2}$ [16]). Again, formula (11) evaluated for the IBM Hamiltonian (5) is peaked just around λ_c , which indicates an increased mixing of the Hamiltonian eigenfunctions in the QPT region. See Refs. [12, 16] for details.

The last analog of specific heat will be elaborated in the rest of this contribution. It originates in the expression

$$\mathcal{U} = - \sum_{i>0} \ln |E_i - E_0| \quad (12)$$

for the ‘‘potential energy’’ of a given set of levels with the same symmetry quantum numbers, as derived from the relation between one-dimensional distributions of charges in a planar universe and analogous distributions of eigenvalues in Gaussian matrix ensembles [30]. This relation, referred to as the static Coulomb-gas analogy, must be distinguished from the dynamical Coulomb-gas analogy, introduced by Pechukas and Yukawa [31], that describes eigenvalue dynamics for Hamiltonians of the form (1).

A quantity proportional to \mathcal{U} in Eq. (12) can be considered as another QPT analog of the thermodynamic potential. In particular, if F_0 is associated with $\mathcal{F}_0 = \Omega^{-1} \lambda \mathcal{U}$, where Ω is a scaling constant that is to be discussed later, the specific heat takes the form

$$\begin{aligned} \mathcal{C} &= - \frac{\lambda}{\Omega} \frac{\partial^2 (\lambda \mathcal{U})}{\partial \lambda^2} = \frac{2\lambda}{\Omega} \sum_{i>0} \left[\frac{\lambda}{2} \left\{ \frac{\frac{\partial^2 E_i}{\partial \lambda^2} - \frac{\partial^2 E_0}{\partial \lambda^2}}{E_i - E_0} - \left(\frac{\frac{\partial E_i}{\partial \lambda} - \frac{\partial E_0}{\partial \lambda}}{E_i - E_0} \right)^2 \right\} + \frac{\frac{dE_i}{d\lambda} - \frac{\partial E_0}{\partial \lambda}}{E_i - E_0} \right] = \\ & \frac{2\lambda^2}{\Omega} \left[\sum_{i>0} \sum_{j \neq i} \frac{|\langle V \rangle_{ij}|^2}{(E_i - E_j)(E_i - E_0)} - \sum_{i>0} \sum_{j>0} \frac{|\langle V \rangle_{0j}|^2}{(E_j - E_0)(E_i - E_0)} - \frac{1}{2} \sum_{i>0} \left(\frac{\langle V \rangle_i - \langle V \rangle_0}{E_i - E_0} \right)^2 + \frac{1}{\lambda} \sum_{i>0} \frac{\langle V \rangle_i - \langle V \rangle_0}{E_i - E_0} \right], \end{aligned} \quad (13)$$

with the last expression resulting from the Pechukas-Yukawa equations [the last two expressions in Eq. (13) are given here just for comparison with Eqs. (10) and (11); from the computational viewpoint the most convenient definition is of course represented by the first formula]. Since the motivation for the proposed relation between \mathcal{F}_0 and \mathcal{U} may be unclear at this moment, we ask the reader for patience till the next section, where the foundation of Eq. (13) will become clear.

It turns out [24] that the specific heat given by the last formula exhibits a form that is very similar to that of Eq. (10). This is illustrated in Figure 1, where specific heat (13) with $\Omega = 1$ is shown for the IBM first- and second-order phase transitions. Since the $N \rightarrow \infty$ limit is numerically inaccessible, we present here only calculations for $N = 10, 20, 40,$ and 80 , corresponding to the curves with increasing height, the maximal values of \mathcal{C} being shown separately in the log-log insets as a function of N . Clearly, the peaks in panel (a) are sharper and higher than those in panel (b), as indeed expected in the first- and second-order phase transition. Moreover, as will be argued below, the inclusion of the right dependence of the scaling Ω on dimension n leads to the correct $N \rightarrow \infty$ asymptotics of Eq. (13). In this case, the specific-heat values at λ_c converge or diverge, respectively, for the IBM second- or first-order QPT’s.

All the above-proposed definitions of specific heat lead to certain sums of squared interaction matrix elements divided by some combinations of energy differences. The observed peaked behavior of these quantities results from the fact that the spectrum becomes more compressed and, simultaneously, also the sum of level interactions get stronger in the phase-transitional region. In fact, we are dealing here with a phenomenon of multiple avoided crossing of levels [10]. The analytic description of such effects can be given in terms of so-called branch points of Hamiltonian (1) in the complex λ plane [32]–[36]. As will be shown below, this description is particularly relevant for the last definition of specific heat in Eq. (13).

BRANCH POINTS AND ZEROS OF PARTITION FUNCTION

Branch, or exceptional points are places in the complex plane of parameter λ where various pairs of eigenvalues of the complex-extended Hamiltonian (1) coalesce [32]. They are simultaneous solutions of equations $\det[E - H(\lambda)] = 0$ and $\frac{\partial}{\partial E} \det[E - H(\lambda)] = 0$, that after elimination yield the condition [33, 35]

$$\mathcal{D} = \prod_k \mathcal{D}_k = (-)^{\frac{n(n-1)}{2}} \prod_{i<j} (E_j - E_i)^2 = 0 \quad (14)$$

with $\mathcal{D}_k = \prod_{i(\neq k)} (E_i - E_k)$. The discriminant \mathcal{D} is a polynomial of order $n(n-1)$ in λ (the dimension of the Hilbert space n being now assumed finite) with real coefficients and its roots thus occur as $\frac{n(n-1)}{2}$ complex conjugate pairs. Except at these points, the complex eigenvalue $E(\lambda)$ obtained from the characteristic polynomial of Hamiltonian (1) is a single analytic function defined on n Riemann sheets. The energy labels in Eq. (14) enumerate the respective

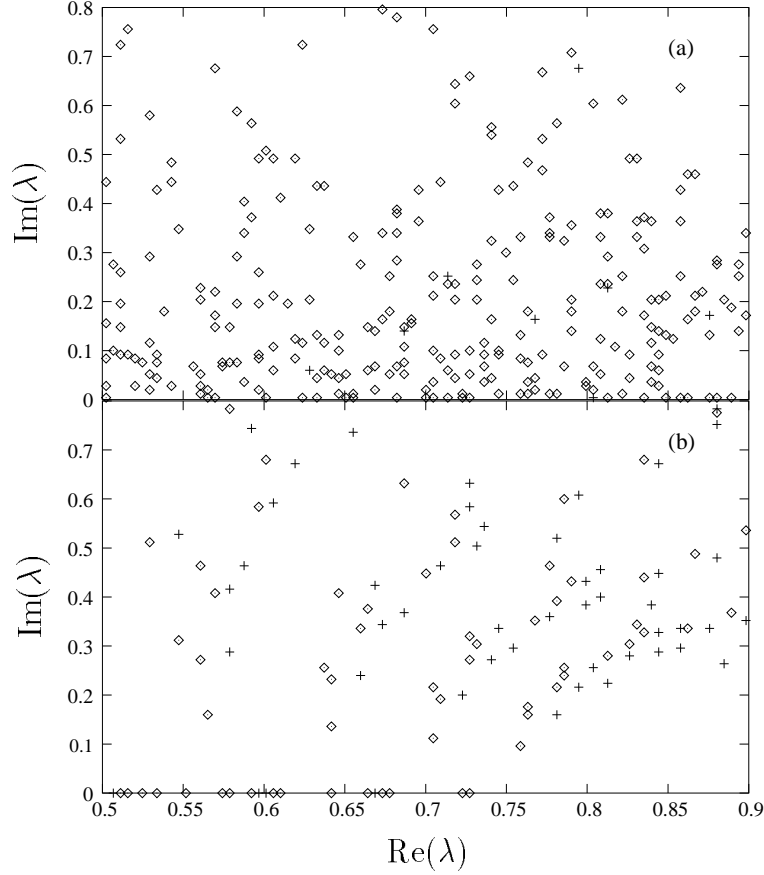


FIGURE 2. Branch points corresponding to all $J = 0$ states for (a) the first-order ($|\chi| = \frac{\sqrt{7}}{2}$) and (b) second-order ($\chi = 0$) QPT paths of the IBM Hamiltonian (5) with $N = 20$. Diamonds represent single branch points and crosses the degenerate ones (within given numerical precision).

Riemann sheet according to the ordering of energies at real λ . The degeneracy points are square-root branch points where the Riemann sheets are pairwise (in generic cases) connected. The leading-order behavior on the two connected sheets close to the branch point λ_b is given by $E(\lambda) - E(\lambda_b) \approx a\sqrt{\lambda - \lambda_b}$ (as a doubly-valued function), with a being a complex constant [6, 34, 35].

The relation of branch points to QPT's has been declared several times—see, e.g., Refs. [6, 10]. Clearly, a branch point located close to the real λ axis affects the local evolution of the corresponding pair of real energies so that the two levels undergo an avoided crossing with accompanying rapid changes of wave functions. A cumulation of branch points close to some real point λ_c thus can give rise to massive structural changes of eigenstates, as observed in QPT's. It moreover turns out that the density of branch points close to λ_c may be determinative for the QPT order, as observed on the real λ axis.

The simplest example can be found in dimension $n = 2$. A general real 2×2 Hamiltonian of the form (1) reads as

$$H(\lambda) = \begin{pmatrix} a_1 + a_2\lambda & c_1 + c_2\lambda \\ c_1 + c_2\lambda & b_1 + b_2\lambda \end{pmatrix}. \quad (15)$$

It is easy to show that the spacing between both eigenvalues $E_1 - E_2 \equiv \Delta E$ behaves according to $|\Delta E| = \sqrt{A + B\lambda + C\lambda^2}$, where the coefficients $A \geq 0$, B , and $C \geq 0$ are some combinations of constants in Eq. (15) such that the value $D = B^2 - 4AC$ is negative. The minimal distance of both levels, $|\Delta E| = \Delta_0 = \sqrt{-\frac{D}{4C}}$, is reached at $\lambda = \lambda_0 = -\frac{B}{2C}$. If λ is extended to the complex plane, one finds that both complex eigenvalues E_1 and E_2 cross in two complex-conjugate branch points $\lambda_{b\pm} = \lambda_0 \pm i\Delta_0$. For Δ_0 converging to zero, the branch points come to the real axis and the avoided crossing turns into a real crossing, implying $|\Delta E| = \sqrt{C}(\lambda - \lambda_b)$. The line that passes both points λ_{b+}

and λ_{b-} in the direction perpendicular to the real axis represents the locus of points where either real or imaginary part of $E_1 - E_2$ vanishes. In particular, one has $\text{Re}\Delta E = 0$ for $|\text{Im}\lambda| \geq |\text{Im}\lambda_{b\pm}|$ and $\text{Im}\Delta E = 0$ for $|\text{Im}\lambda| \leq |\text{Im}\lambda_{b\pm}|$. Only at $\lambda = \lambda_{b\pm}$ both loci overlap so that at these points $\text{Re}\Delta E = \text{Im}\Delta E = 0$. This corresponds to the above-mentioned behavior of the complex square root (valid for $\Delta_0 > 0$).

In the $n = 2$ case, the domain of $E(\lambda)$ consists of two Riemann sheets only. It is evident that the analysis becomes much more complicated for higher dimensions. Methods to locate individual branch points in the complex plane for arbitrary n were developed (see, e.g., Ref. [33]), but without the knowledge of explicit Riemann sheet structure of the specific problem one cannot select those branch points that are located on the ground-state sheet. An example is shown in Figure 2. Here, branch points corresponding to the $J = 0$ submatrix of the IBM Hamiltonian (5) with $N = 20$ are shown for the first-order QPT with $\chi = \pm \frac{\sqrt{7}}{2}$ (panel a) and for second-order transition, $\chi = 0$ (panel b). The distributions in both panels show no cumulation of branch points near the respective critical points $\lambda_c = 0.8181 \dots$ (a) and $\lambda_c = 0.8$ (b), which reflects the fact that all Riemann sheets are mixed together.

As can be observed, some of the branch points in panel (a) of Fig. 2 come very close to the real axis, but the absence of additional integrals of motions in the $\chi \neq 0$ transitional regimes guarantees that $\text{Im}\lambda_b \neq 0$ in all these cases. On the other hand, several branch points in panel (b) are located exactly on the real axis, with $\text{Im}\lambda_b = 0$, which seems to contradict the familiar no-crossing rule. Indeed, the $\chi = 0$ transitional path is not quite generic since the underlying $O(5)$ dynamical symmetry of the $O(6)$ and $U(5)$ limits remains unbroken and gives rise to the seniority quantum number ν , that is valid along the whole transition [37]. Consequently, levels with different ν 's can cross without repulsion. It must be stressed, however, that none of these very close avoided (panel a) or unavoided (panel b) crossings is related to the ground-state Riemann sheet.

In generic cases, the determination of the Riemann sheet structure in its full complexity is prohibitively difficult even for moderate dimensions. The loci of $\text{Re}\Delta E = 0$ and $\text{Im}\Delta E = 0$ crossings are not any more straight lines, as for $n = 2$, but generate complicated patterns that can be hardly disentangled having only a finite numerical precision. (Nevertheless, the $\text{Re}\Delta E = 0$ curves for IBM form a flow with prevailing perpendicular orientation toward the real λ axis, see the preprint in Ref. [24].) As a consequence, practically nothing is known about the density of the ground-state branch points in a vicinity of λ_c for QPT's of various orders.

We will show that the specific heat in Eq. (13), although depending solely on the real- λ observables, represents an *indirect measure* of the density of branch points on the ground-state Riemann sheet near the real axis. To prove this, we start from following question: If $\mathcal{F}_0 = \Omega^{-1} \lambda \mathcal{U}$ represents the equilibrium value of the “free energy”, as assumed above, what is the corresponding “partition function” \mathcal{Z} ? Using the thermodynamic relation $F_0 = -T \ln Z$, one finds

$$\mathcal{Z}^\Omega = \prod_{i>0} (E_i - E_0), \quad (16)$$

thus \mathcal{Z} coincides with the Ω^{-1} th power of the partial discriminant \mathcal{D}_0 from Eq. (14). Recall that the square \mathcal{D}_k^2 is a polynomial in λ with $n - 1$ complex conjugate pairs of roots, each of them being simultaneously assigned to one other \mathcal{D}_k^2 . These roots correspond to the branch points located on the k -th Riemann sheet. Thus branch points on the ground-state Riemann sheet are zeros of the fictitious partition function \mathcal{Z} , that generates the specific heat in Eq. (13).

Zeros of canonical or grand canonical partition functions Z in complex temperatures and/or chemical potentials play an essential role in the fundamental theory of thermodynamic phase transitions. Indeed, as noticed by Yang and Lee [26], for a system of particles with mass m interacting through a potential with a hard repulsive core the grand partition function Z can be written as a polynomial in the parameter $y = (\hbar^{-1} \sqrt{mT})^3 \exp(T^{-1}\mu)$, containing both temperature T and chemical potential μ . While for a finite size of the system the roots of $Z(y)$ must keep away from the real y axis, in the thermodynamic limit there may exist places where the zeros approach infinitely close to the real axis, giving rise to a phase transition at the given value y_c . This method was adapted also for canonical ensembles [27], where it was shown that the density of zeros of the partition function close to the phase-transitional temperature T_c even determines the order of the transition, as reflected by the behavior of standard thermodynamic specific heat.

This was recently proposed [38] as a basis for phase-transitional analyses in small systems. For instance, if zeros of Z are located along a curve crossing the real axis and if the closest zero converges to a real point T_c in the thermodynamic limit, the order of the corresponding phase transition at T_c is determined by (i) the power α in the dependence $\rho \propto (\text{Im}T)^\alpha$ of the density of zeros close to the real axis, and by (ii) the angle ν between the $Z = 0$ domain and the normal to real axis [38]. Namely, the phase transition will be of the first order for $\alpha = \nu = 0$, of the second order for $\alpha \in (0, 1]$, and of a higher order for $\alpha > 1$. A detailed analysis of even more possibilities can be found in Ref. [27].

Because the “specific heat” (13) results—as we know now—from the “partition function” (16), it basically measures the density of zeros of \mathcal{Z} near the real λ axis, or, in other words, the density of branch points on the ground-state

Riemann sheet. The peaked behaviors shown in Fig. 1 thus indicate that the IBM g.s. branch points indeed accumulate near λ_c for $N \rightarrow \infty$, and that the degree of this accumulation differs for transitions of different orders. We are now in a position to formulate the central statement of this contribution, namely, the surmise [24] that *the κ th-order QPT distribution of the ground-state branch points is quantitatively similar to a distribution of the $Z(T)$ complex zeros in a thermodynamic phase transition of the same order κ .*

NORMALIZATION AND LARGE-N ASYMPTOTICS

To test the conjecture proposed at the end of the last section, we need to discuss the factor Ω , that appears in Eqs. (13) and (16). In fact, this factor should not be a constant, but a certain function depending on the system's size (quite similarly to the standard specific heat, which must be normalized to a unit part of the thermodynamic system). Since the polynomial \mathcal{D}_0^2 is determined (up to a multiplicative constant) by its complex roots, one may express specific heat (13) as an integral containing the density $\rho_0(\lambda) = \sum_i \delta(\lambda - \lambda_{bi})$ of the branch points λ_{bi} on the g.s. Riemann sheet [24]. The normalization of $\int \rho_0 d\lambda$ to unity yields a factor $\propto (n-1)^{-1}$ (there are $n-1$ branch points on each Riemann sheet) and one arrives at the formula

$$\Omega = \Omega_0(n-1), \quad (17)$$

where n is the relevant Hilbert space dimension and Ω_0 an arbitrary constant. Eq. (17) is analogous to the scaling based on the grand partition function, as discussed by Yang and Lee [26], since in that case the order of the polynomial $Z(y)$ equals to N_{\max} , the maximal number of particles in a given volume, and $\Omega \propto N_{\max}$ can be identified with the volume.

In the IBM, the total number of states grows roughly as $\sim N^5/120$ for very large boson numbers (if not counting the rotational degeneracy). However, the dimension of the $J=0$ subspace, which is relevant in the calculation leading to Fig. 1, is given by $n \sim N^2/12$. So the correct normalization of Eq. (13) in the IBM case is by a factor $\Omega \propto N^2$. Figure 3 shows—by the curve demarcated by squares—the maximal values of such normalized specific heat in the second-order ($\chi=0$) QPT region for very high boson numbers N . Note that such high-dimensional calculation were enabled by the underlying $O(5)$ dynamical symmetry at $\chi=0$, so they could not be performed for the other transitional path (a). The algebraic increase shown for $N \leq 80$ in the inset of Fig. 1(b) (calculated for $\Omega=1$) represents only the initial part of the curve in Fig. 3, where the convergence to the $A \propto N^2$ asymptotics is evident for $N > 300$. For comparison, the convergence of the maximal value of specific heat (10) to its asymptotic value (which is for $\chi=0$ equal to 12.5) is also shown in Fig. 3 by full circles. Clearly, the degree of convergence in both cases (squares and circles) is about the same. On the other hand, since the $N \leq 80$ increase observed in panel (a) of Fig. 1 is much faster than the increase in panel (b), one expects that the asymptotic increase of the maximal \mathcal{C} value in the first-order QPT is faster than $A \propto N^2$ (although in this case the $N > 100$ region is numerically inaccessible). This indicates that the QPT behavior of the specific heat (13) is consistent with the behavior of the standard specific heat in the first- and second-order thermodynamic phase transitions, in agreement with the above proposed conjecture [24].

This conclusion is also supported by the analysis of the $N \rightarrow \infty$ limit. Indeed, due to the degeneracy of $\beta_0 = 0$ and $\beta_0 \neq 0$ minima of the function (7) at λ_c for $\chi \neq 0$, there will be a branch point on g.s. Riemann sheet that asymptotically reaches the real axis. In contrast, there is no actual ground-state involving degeneracy in the $N \rightarrow \infty$ limit of the second-order transition, although, as can be shown, exceptional points come infinitely close to the real axis at the critical point.

Let us stress that in calculations leading to the above-discussed results all levels with $J=0$ were included in Eq. (13). We know, however, that for $\chi=0$ some pairs of levels actually cross at real λ (due to the seniority quantum number), which implies that first and second derivatives of the corresponding energies may be discontinuous or diverging. Fortunately, a detailed consideration of this problem reveals that all these singularities cancel out exactly and do not affect the shapes of curves in Figs. 1(b) and 3. Indeed, if E_i crosses with E_{i+1} , the discontinuity (singularity) of the first (second) derivatives in Eq. (13) for both levels is the same, but with opposite signs, so the sum of both contributions is incremented correctly, as if the levels continuously passed the crossing.

In any case, one can repeat all $\chi=0$ calculations including only the $v=0$ subspace of states with $J=0$ into expression (13). Since this subspace contains the ground state and does not mix with $v \neq 0$ subspaces, one obtains a plausible new definition of the $\chi=0$ specific heat, which avoids the above-discussed problem with singularities. The dimension of the $v=0$ subspace grows as $n \sim N/2$, thus $\Omega \propto N$. Maximal values of the resulting specific heat curves with this normalization are shown in Fig. 3 by triangles. We observe a similar dependence as before, but because of lower dimensions the convergence with N is much slower now than before, not allowing a fully conclusive evidence of finite asymptotics. The available data for boson numbers up to 5000 (see the inset in Fig. 3) are consistent with

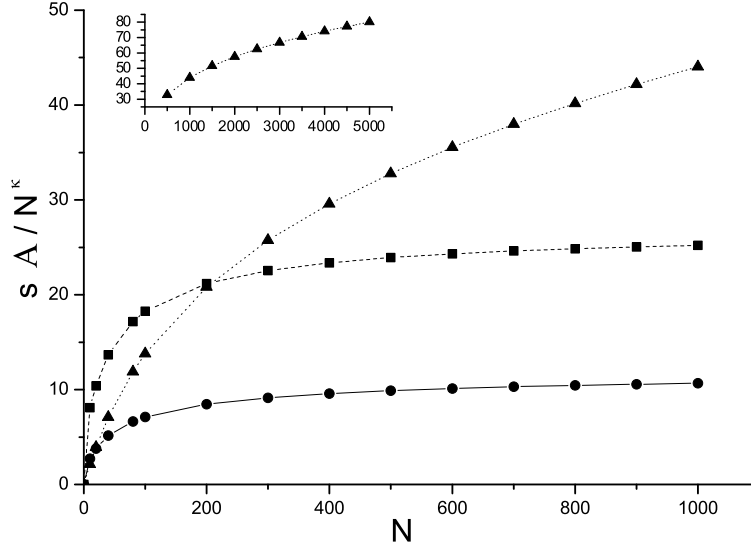


FIGURE 3. Maximal values of specific heat (13) (squares and triangles) normalized according to Eq. (17) in the IBM second-order QPT ($\chi = 0$) for very large boson numbers. Squares (or triangles) correspond to the inclusion of the whole $J = 0$ space (or its $\nu = 0$ subspace) into the sum in Eq. (13). Different (arbitrary) scaling factors were used to show both sets of data within the same range. For comparison, the convergence of the maximal value of specific heat (10) to its asymptotic limit $A_\infty = 12.5$ is shown by full circles.

large- N behaviors given by $A \propto N^k$ for $k \in (0, 1.35)$, in agreement with the expected value $k = 1$. Let us stress that the dimension n of the $\nu = 0$ subspace at $N = 5000$ is comparable with the dimension of the whole $J = 0$ subspace at $N \approx 170$, so the absence of saturation in the $\nu = 0$ case in the available domain of boson numbers is not surprising. To obtain $\nu = 0$ results comparable with $J = 0$ at $N \approx 300$, one would need to go up to $N \approx 15000$, which is beyond our present computational possibilities.

CONCLUSIONS AND OUTLOOK

We have discussed several aspects of quantum structural phase transitions at zero temperature that could eventually lead to their unified description with classical thermodynamic phase transitions. The most fundamental aspect seems to follow from the analogy [24] between the branch points related to the ground-state Riemann-sheet of Hamiltonian (1) and complex zeros of the partition function of a classical phase-transitional system. Numerical data strongly supporting this conjecture were obtained in the interacting boson model, although a fully conclusive test would require to further increase the upper limit of available boson numbers. The immediate next task is to extend the calculations presented here to other systems that exhibit quantum phase transitions of various orders.

An open problem is the generalization of our approach to finite temperatures. In this case, both structural and thermodynamic phase transitions describe nonanalytic behaviors of the thermodynamic potential $F_0(\lambda, T)$ along two perpendicular directions in the $\lambda \times T$ parameter space. While the T -direction is described by standard thermodynamics, involving the theory of complex zeros of the partition function, the λ -direction is not as familiar. Formula (3) represents a possible starting point of the analysis. The finite-temperature average of V' is just a weighted sum of averages corresponding to individual excited states

$$\langle V' \rangle_T = \frac{1}{Z} \sum_i e^{-T^{-1} E_i} \langle V' \rangle_i \quad (18)$$

and one can ask whether a thermally weighted sum ρ_T of branch-point densities ρ_i on the Riemann sheets assigned to excited states will, in the finite- T case, take the role of the g.s. density ρ_0 , as discussed above.

The interacting boson model seems to be an ideal tool for studying various aspects of complex quantum dynamics, including quantum phase transitions. One of its advantages in this respect is the presence of quantum phase transitions

of both first and second orders. We consider this model as one of the best candidates also for future finite-temperature studies.

ACKNOWLEDGMENTS

P.C. and S.H. thank Jan Jolie for relevant discussions. This work was supported by GAČR and ASČR under Project Nos. 202/02/0939 and K1048102, respectively, and by the DFG under Grant No. 436 TSE 17/6/03.

REFERENCES

1. S. Sachdev, *Quantum Phase Transitions* (Cambridge University Press, Cambridge, UK, 1999).
2. R. Gilmore, *Catastrophe Theory for Scientists and Engineers* (Wiley, New York, 1981).
3. A.E.L. Dieperink, O. Scholten, and F. Iachello, Phys. Rev. Lett. **44**, 1747 (1980).
4. D.H. Feng, R. Gilmore, and S.R. Deans, Phys. Rev. C **23**, 1254 (1981).
5. W.-M. Zhang, D.H. Feng, and J.N. Ginocchio, Phys. Rev. Lett. **59**, 2032 (1987).
6. W.D. Heiss, Z. Phys. A - Atomic Nuclei **329**, 133 (1988); W.D. Heiss and A.L. Sannino, Phys. Rev. A **43**, 4159 (1991); W.D. Heiss, Phys. Rep. **242**, 443 (1994).
7. E. López-Moreno and O. Castaños, Phys. Rev. C **54**, 2374 (1996).
8. D.J. Rowe, C. Bahri, and W. Wijesundera, Phys. Rev. Lett. **80**, 4394 (1998).
9. R.F. Casten, D. Kusnezov, and N.V. Zamfir, Phys. Rev. Lett. **82**, 5000 (1999).
10. P. Cejnar and J. Jolie, Phys. Rev. E **61**, 6237 (2000).
11. F. Iachello, Phys. Rev. Lett. **85**, 3580 (2000); *ibid.* **87**, 052502 (2001).
12. P. Cejnar, V. Zelevinsky, and V.V. Sokolov, Phys. Rev. E **63**, 036127 (2001).
13. J. Jolie, R.F. Casten, P. von Brentano, and V. Werner, Phys. Rev. Lett. **87**, 162501 (2001).
14. J. Jolie, P. Cejnar, R.F. Casten, S. Heinze, A. Linnemann, and V. Werner, Phys. Rev. Lett. **89**, 182502 (2002).
15. P. Cejnar, Phys. Rev. Lett. **90**, 112501 (2003).
16. P. Cejnar, S. Heinze, and J. Jolie, Phys. Rev. C **68**, 034326 (2003).
17. A. Volya and V. Zelevinsky, Phys. Lett. B **574**, 27 (2003).
18. C. Emary and T. Brandes, Phys. Rev. Lett. **90**, 044101 (2003); N. Lambert, C. Emary, T. Brandes, *ibid.* **92**, 073602 (2004).
19. J.M. Arias, J. Dukelsky, and J.E. García-Ramos, Phys. Rev. Lett. **91**, 162502 (2003).
20. F. Iachello and N.V. Zamfir, Phys. Rev. Lett. **92**, 212501 (2004).
21. J. Jolie, S. Heinze, P. Van Isacker, and R.F. Casten, Phys. Rev. C **70**, 011305(R) (2004).
22. D.J. Rowe, Phys. Rev. Lett. **93**, 122502 (2004); D.J. Rowe, P.S. Turner, and G. Rosensteel, *ibid.* **93**, 232502 (2004).
23. J.M. Arias, J.E. García-Ramos, and J. Dukelsky, Phys. Rev. Lett. **93**, 212501 (2004); M.A. Caprio and F. Iachello, *ibid.* **93**, 242502 (2004).
24. P. Cejnar, S. Heinze, and J. Dobeš, Phys. Rev. C in press (2005); see also nucl-th/0406060.
25. V. Zelevinsky and A. Volya, Phys. Rep. **391**, 311 (2004).
26. C.N. Yang and T.D. Lee, Phys. Rev. **87**, 404 (1952); **87**, 410 (1952).
27. S. Grossmann and W. Rosenhauer, Z. Phys. **207**, 138 (1967); **218**, 437 (1969); S. Grossmann and V. Lehmann, *ibid.* **218**, 449 (1969).
28. F. Iachello, A. Arima, *The Interacting Boson Model* (Cambridge University Press, Cambridge, UK, 1987).
29. J.N. Ginocchio and M.V. Kirson, Nucl. Phys. **A350**, 31 (1980).
30. F.J. Dyson, J. Math. Phys. **3**, 140 (1962).
31. P. Pechukas, Phys. Rev. Lett. **51**, 943 (1983); T. Yukawa, *ibid.* **54**, 1883 (1985).
32. T. Kato, *Perturbation Theory for Linear Operators* (Springer, Berlin, 1966).
33. M.R. Zirnbauer, J.J.M. Verbaarschot, and H.A. Weidenmüller, Nucl. Phys. **A411**, 161 (1983).
34. P.E. Shanley, Ann. Phys. **186**, 292 (1988).
35. W.D. Heiss and W.-H. Steeb, J. Math. Phys. **32**, 3003 (1991).
36. I. Rotter, Phys. Rev. C **64**, 034301 (2001); I. Rotter and A.F. Sadreev, Phys. Rev. E **69**, 066201 (2004).
37. A. Leviatan, A. Novoselsky, and I. Talmi, Phys. Lett. B **172**, 144 (1986).
38. P. Borrmann, O. Mülken, and J. Harting, Phys. Rev. Lett. **84**, 3511 (2000); O. Mülken, H. Stamerjohanns, and P. Borrmann, Phys. Rev. E **64**, 047105 (2001).